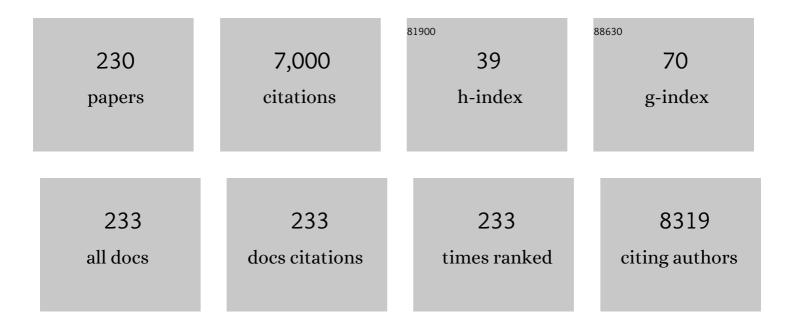
Xiaohua Lu

List of Publications by Year in descending order

Source: https://exaly.com/author-pdf/2033408/publications.pdf Version: 2024-02-01



#	Article	IF	CITATIONS
1	Anaerobic co-digestion process for biogas production: Progress, challenges and perspectives. Renewable and Sustainable Energy Reviews, 2017, 76, 1485-1496.	16.4	590
2	The peculiar effect of water on ionic liquids and deep eutectic solvents. Chemical Society Reviews, 2018, 47, 8685-8720.	38.1	346
3	Bioinspired Graphene Nanopores with Voltage-Tunable Ion Selectivity for Na ⁺ and K ⁺ . ACS Nano, 2013, 7, 10148-10157.	14.6	199
4	Enhanced Photocatalytic Activity in Anatase/TiO ₂ (B) Coreâ^'Shell Nanofiber. Journal of Physical Chemistry C, 2008, 112, 20539-20545.	3.1	181
5	Effect of Water on the Density, Viscosity, and CO ₂ Solubility in Choline Chloride/Urea. Journal of Chemical & Engineering Data, 2014, 59, 3344-3352.	1.9	170
6	Molecular dynamics study on ionic hydration. Fluid Phase Equilibria, 2002, 194-197, 257-270.	2.5	161
7	An enhanced CdS/TiO2 photocatalyst with high stability and activity: Effect of mesoporous substrate and bifunctional linking molecule. Journal of Materials Chemistry, 2011, 21, 4945.	6.7	156
8	Choline-based deep eutectic solvents for CO2 separation: Review and thermodynamic analysis. Renewable and Sustainable Energy Reviews, 2018, 97, 436-455.	16.4	134
9	Anomalous Hydration Shell Order of Na ⁺ and K ⁺ inside Carbon Nanotubes. Nano Letters, 2009, 9, 989-994.	9.1	113
10	Highly Thermal Stable and Highly Crystalline Anatase TiO ₂ for Photocatalysis. Environmental Science & Technology, 2009, 43, 5423-5428.	10.0	103
11	CuO/Cu ₂ O porous composites: shape and composition controllable fabrication inherited from metal organic frameworks and further application in CO oxidation. Journal of Materials Chemistry A, 2015, 3, 5294-5298.	10.3	100
12	Screening of conventional ionic liquids for carbon dioxide capture and separation. Applied Energy, 2016, 162, 1160-1170.	10.1	93
13	Construction of Hierarchically Porous Nanoparticles@Metal–Organic Frameworks Composites by Inherent Defects for the Enhancement of Catalytic Efficiency. Advanced Materials, 2018, 30, e1803263.	21.0	88
14	Core–shell TiO2/C nanofibers as supports for electrocatalytic and synergistic photoelectrocatalytic oxidation of methanol. Journal of Materials Chemistry, 2012, 22, 4025.	6.7	83
15	Energy consumption analysis for CO2 separation using imidazolium-based ionic liquids. Applied Energy, 2014, 136, 325-335.	10.1	78
16	Stability of Pt nanoparticles and enhanced photocatalytic performance in mesoporous Pt-(anatase/TiO2(B)) nanoarchitecture. Journal of Materials Chemistry, 2009, 19, 7055.	6.7	72
17	Wellâ€Dispersed and Sizeâ€Controlled Supported Metal Oxide Nanoparticles Derived from MOF Composites and Further Application in Catalysis. Small, 2015, 11, 3130-3134.	10.0	70
18	Solubilities of CO2, CH4, H2, CO and N2 in choline chloride/urea. Green Energy and Environment, 2016, 1, 195-200.	8.7	65

#	Article	IF	CITATIONS
19	Thermodynamic Study of Choline Chloride-Based Deep Eutectic Solvents with Water and Methanol. Journal of Chemical & Engineering Data, 2020, 65, 2446-2457.	1.9	65
20	Study on the formation and growth of potassium titanate whiskers. Journal of Materials Science, 2002, 37, 3035-3043.	3.7	64
21	Ice-like Water Structure in Carbon Nanotube (8,8) Induces Cationic Hydration Enhancement. Journal of Physical Chemistry C, 2013, 117, 11412-11420.	3.1	64
22	Water on Titanium Dioxide Surface: A Revisiting by Reactive Molecular Dynamics Simulations. Langmuir, 2014, 30, 14832-14840.	3.5	64
23	Techno-economic analysis and performance comparison of aqueous deep eutectic solvent and other physical absorbents for biogas upgrading. Applied Energy, 2018, 225, 437-447.	10.1	60
24	Diffusion of water molecules confined in slits of rutile TiO2(110) and graphite(0001). Fluid Phase Equilibria, 2011, 302, 316-320.	2.5	59
25	A New Electrochemical System Based on a Flow-Field Shaped Solid Electrode and 3D-Printed Thin-Layer Flow Cell: Detection of Pb ²⁺ lons by Continuous Flow Accumulation Square-Wave Anodic Stripping Voltammetry. Analytical Chemistry, 2017, 89, 5024-5029.	6.5	59
26	Molecular Dynamics Study of Mg ²⁺ /Li ⁺ Separation via Biomimetic Graphene-Based Nanopores: The Role of Dehydration in Second Shell. Langmuir, 2016, 32, 13778-13786.	3.5	58
27	Metal–Organic Framework Derivatives for Improving the Catalytic Activity of the CO Oxidation Reaction. ACS Applied Materials & Interfaces, 2017, 9, 15394-15398.	8.0	53
28	Facile Synthesis of Mesoporous MoS ₂ â€TiO ₂ Nanofibers for Ultrastable Lithium Ion Battery Anodes. ChemElectroChem, 2015, 2, 374-381.	3.4	51
29	Structurally tuning microwave absorption of core/shell structured CNT/polyaniline catalysts for energy efficient saccharide-HMF conversion. Applied Catalysis B: Environmental, 2018, 220, 581-588.	20.2	50
30	Elastic interlayer toughening of potassium titanate whiskers-nylon66 composites and their fractal research. Journal of Applied Polymer Science, 2001, 82, 368-374.	2.6	49
31	Molecular simulations on nanoconfined water molecule behaviors for nanoporous material applications. Microfluidics and Nanofluidics, 2013, 15, 191-205.	2.2	49
32	Molecular Dynamics Study on Diameter Effect in Structure of Ethanol Molecules Confined in Single-Walled Carbon Nanotubesâ€. Journal of Physical Chemistry C, 2007, 111, 15677-15685.	3.1	48
33	Carbon titania mesoporous composite whisker as stable supercapacitor electrode material. Journal of Materials Chemistry, 2010, 20, 7645.	6.7	47
34	Thermodynamic Study for Gas Absorption in Choline-2-pyrrolidine-carboxylic Acid + Polyethylene Glycol. Journal of Chemical & Engineering Data, 2016, 61, 3428-3437.	1.9	47
35	High Quality and Yield in Potassium Titanate Whiskers Synthesized by Calcination from Hydrous Titania. Journal of the American Ceramic Society, 2004, 87, 326-330.	3.8	45
36	Experimental study of CO 2 absorption in aqueous cholinium-based ionic liquids. Fluid Phase Equilibria, 2017, 445, 14-24.	2.5	45

#	Article	lF	CITATIONS
37	Carbon heterogeneous surface modification on a mesoporous TiO2-supported catalyst and its enhanced hydrodesulfurization performance. Chemical Communications, 2012, 48, 11525.	4.1	43
38	Modeling thermodynamic derivative properties of ionic liquids with ePC-SAFT. Fluid Phase Equilibria, 2015, 405, 73-82.	2.5	43
39	TiO2 nanofibers heterogeneously wrapped with reduced graphene oxide as efficient Pt electrocatalyst supports for methanol oxidation. International Journal of Hydrogen Energy, 2015, 40, 3679-3688.	7.1	42
40	Comparative Study of Tribological Properties of Different Fibers Reinforced PTFE/PEEK Composites at Elevated Temperatures. Tribology Transactions, 2010, 53, 189-194.	2.0	41
41	Melting and Freezing of Au Nanoparticles Confined in Armchair Single-Walled Carbon Nanotubes. Journal of Physical Chemistry C, 2010, 114, 2896-2902.	3.1	41
42	Coupled Chemical and Thermal Drivers in Microwaves toward Ultrafast HMF Oxidation to FDCA. ACS Sustainable Chemistry and Engineering, 2018, 6, 11493-11501.	6.7	41
43	Techno-economic analysis of biomass processing with dual outputs of energy and activated carbon. Bioresource Technology, 2021, 319, 124108.	9.6	41
44	Molecular Simulation Study of the Adsorption and Diffusion of a Mixture of CO ₂ /CH ₄ in Activated Carbon: Effect of Textural Properties and Surface Chemistry. Journal of Chemical & Engineering Data, 2016, 61, 4139-4147.	1.9	40
45	Modeling, simulation and evaluation of biogas upgrading using aqueous choline chloride/urea. Applied Energy, 2018, 229, 1269-1283.	10.1	40
46	Molecular insights into multilayer 18-crown-6-like graphene nanopores for K+/Na+ separation: A molecular dynamics study. Carbon, 2019, 144, 32-42.	10.3	40
47	Tribological and mechanical properties of carbon-nanofiber-filled polytetrafluoroethylene composites. Journal of Applied Polymer Science, 2007, 104, 2430-2437.	2.6	38
48	Excellent performance of Pt-C/TiO 2 for methanol oxidation: Contribution of mesopores and partially coated carbon. Applied Surface Science, 2017, 426, 890-896.	6.1	38
49	Mg ²⁺ -Channel-Inspired Nanopores for Mg ²⁺ /Li ⁺ Separation: The Effect of Coordination on the Ionic Hydration Microstructures. Langmuir, 2017, 33, 9201-9210.	3.5	38
50	A shortcut for evaluating activities of TiO2 facets: water dissociative chemisorption on TiO2-B (100) and (001). Physical Chemistry Chemical Physics, 2010, 12, 8721.	2.8	37
51	Effect of water concentration on the microstructures of choline chloride/urea (1:2) /water mixture. Fluid Phase Equilibria, 2018, 470, 134-139.	2.5	37
52	Improving high-pressure water scrubbing through process integration and solvent selection for biogas upgrading. Applied Energy, 2020, 276, 115462.	10.1	37
53	Enriching Heteroelements in Lignin as Lubricating Additives for Bioionic Liquids. ACS Sustainable Chemistry and Engineering, 2016, 4, 3877-3887.	6.7	36
54	Evaluation of imidazolium-based ionic liquids for biogas upgrading. Applied Energy, 2016, 175, 69-81.	10.1	36

#	Article	IF	CITATIONS
55	Tribological properties of PTFE composites filled with surface-treated carbon fiber. Journal of Materials Science, 2007, 42, 8465-8469.	3.7	35
56	Facile synthesis of amino-functionalized mesoporous TiO 2 microparticles for adenosine deaminase immobilization. Microporous and Mesoporous Materials, 2017, 239, 158-166.	4.4	35
57	A controllable approach for the synthesis of titanate derivatives of potassium tetratitanate fiber. Journal of Materials Science, 2004, 39, 3745-3750.	3.7	34
58	Molecular behavior of water in TiO2 nano-slits with varying coverages of carbon: a molecular dynamics simulation study. Physical Chemistry Chemical Physics, 2012, 14, 16536.	2.8	34
59	Massâ€ŧransfer rate enhancement for CO ₂ separation by ionic liquids: Theoretical study on the mechanism. AICHE Journal, 2015, 61, 4437-4444.	3.6	34
60	Niobium-doped TiO2 solid acid catalysts: Strengthened interfacial polarization, amplified microwave heating and enhanced energy efficiency of hydroxymethylfurfural production. Applied Catalysis B: Environmental, 2019, 243, 741-749.	20.2	34
61	A template-free method for stable CuO hollow microspheres fabricated from a metal organic framework (HKUST-1). Nanoscale, 2015, 7, 9411-9415.	5.6	33
62	Modeling Thermodynamic Derivative Properties and Gas Solubility of Ionic Liquids with ePC-SAFT. Industrial & Engineering Chemistry Research, 2019, 58, 8401-8417.	3.7	33
63	Modeling the Viscosity of Ionic Liquids with the Electrolyte Perturbed-Chain Statistical Association Fluid Theory. Industrial & amp; Engineering Chemistry Research, 2014, 53, 20258-20268.	3.7	32
64	Enhancing Energy Efficiency in Saccharide–HMF Conversion with Core/shell Structured Microwave Responsive Catalysts. ACS Sustainable Chemistry and Engineering, 2017, 5, 4352-4358.	6.7	32
65	Water in Narrow Carbon Nanotubes: Roughness Promoted Diffusion Transition. Journal of Physical Chemistry C, 2018, 122, 19124-19132.	3.1	32
66	Single-crystalline and reactive facets exposed anatase TiO2 nanofibers with enhanced photocatalytic properties. Journal of Materials Chemistry, 2011, 21, 6718.	6.7	31
67	TiO2-B nanofibers with high thermal stability as improved anodes for lithium ion batteries. Electrochemistry Communications, 2013, 27, 124-127.	4.7	31
68	A hybrid perturbed-chain SAFT density functional theory for representing fluid behavior in nanopores. Journal of Chemical Physics, 2013, 138, 224706.	3.0	31
69	Energy consumption analysis for CO2 separation from gas mixtures. Applied Energy, 2014, 130, 237-243.	10.1	31
70	Bovine Serum Albumin Adsorption in Mesoporous Titanium Dioxide: Pore Size and Pore Chemistry Effect. Langmuir, 2016, 32, 3995-4003.	3.5	31
71	Liquid–Solid Nanofriction and Interfacial Wetting. Langmuir, 2016, 32, 743-750.	3.5	31
72	A hybrid perturbed-chain SAFT density functional theory for representing fluid behavior in nanopores: Mixtures. Journal of Chemical Physics, 2013, 139, 194705.	3.0	30

#	Article	IF	CITATIONS
73	Molar Enthalpy of Mixing for Choline Chloride/Urea Deep Eutectic Solvent + Water System. Journal of Chemical & Engineering Data, 2016, 61, 4172-4177.	1.9	30
74	Low-temperature controllable calcination syntheses of potassium dititanate. AICHE Journal, 2004, 50, 1568-1577.	3.6	29
75	A Simple Prediction Model for Higher Heat Value of Biomass. Journal of Chemical & Engineering Data, 2016, 61, 4039-4045.	1.9	29
76	Effect of Adsorbed Alcohol Layers on the Behavior of Water Molecules Confined in a Graphene Nanoslit: A Molecular Dynamics Study. Langmuir, 2017, 33, 11467-11474.	3.5	29
77	Carbon recycling – An immense resource and key to a smart climate engineering: A survey of technologies, cost and impurity impact. Renewable and Sustainable Energy Reviews, 2020, 131, 110010.	16.4	29
78	Modeling Viscosity of Ionic Liquids with Electrolyte Perturbed-Chain Statistical Associating Fluid Theory and Free Volume Theory. Industrial & Engineering Chemistry Research, 2018, 57, 8784-8801.	3.7	28
79	Molecular Dynamics Study of Pore Inner Wall Modification Effect in Structure of Water Molecules Confined in Single-Walled Carbon Nanotubes. Journal of Physical Chemistry C, 2009, 113, 882-889.	3.1	25
80	Friction and Wear Behavior of CF/PTFE Composites Lubricated by Choline Chloride Ionic Liquids. Tribology Letters, 2013, 49, 413-420.	2.6	25
81	Carbon-protected Au nanoparticles supported on mesoporous TiO ₂ for catalytic reduction of p-nitrophenol. RSC Advances, 2014, 4, 29591-29594.	3.6	25
82	Mass Transfer Rate Enhancement for CO2 Separation by Ionic Liquids: Effect of Film Thickness. Industrial & Engineering Chemistry Research, 2016, 55, 366-372.	3.7	25
83	Molecular Interactions of Protein with TiO ₂ by the AFM-Measured Adhesion Force. Langmuir, 2017, 33, 11626-11634.	3.5	25
84	Adjusting the rheological properties of corn-straw slurry to reduce the agitation power consumption in anaerobic digestion. Bioresource Technology, 2019, 272, 360-369.	9.6	25
85	Non-equilibrium thermodynamics analysis and its application in interfacial mass transfer. Science China Chemistry, 2011, 54, 1659-1666.	8.2	24
86	Wetting Behavior of Ionic Liquid on Mesoporous Titanium Dioxide Surface by Atomic Force Microscopy. ACS Applied Materials & Interfaces, 2013, 5, 2692-2698.	8.0	24
87	Review on heat-utilization processes and heat-exchange equipment in biogas engineering. Journal of Renewable and Sustainable Energy, 2016, 8, .	2.0	24
88	Determination of dissolution kinetics of K2SO4 crystal with ion selective electrode. Chemical Engineering Science, 2001, 56, 7017-7024.	3.8	23
89	Theoretical Investigation of CO Adsorption on Clean and Hydroxylated TiO ₂ -B (100) Surfaces. Journal of Physical Chemistry C, 2011, 115, 8622-8629.	3.1	23
90	Controllable atomistic graphene oxide model and its application in hydrogen sulfide removal. Journal of Chemical Physics, 2013, 139, 194707.	3.0	23

#	Article	IF	CITATIONS
91	CO 2 /N 2 separation using supported ionic liquid membranes with green and cost-effective [Choline][Pro]/PEG200 mixtures. Chinese Journal of Chemical Engineering, 2016, 24, 1513-1521.	3.5	23
92	Physicochemical properties and structure of fluid at nano-/micro-interface: Progress in simulation and experimental study. Green Energy and Environment, 2020, 5, 274-285.	8.7	23
93	Reaction and Crystallization Mechanism of Potassium Dititanate Fibers Synthesized by Low-Temperature Calcination. Crystal Growth and Design, 2005, 5, 1399-1404.	3.0	22
94	Modelling of mass transfer coupling with crystallization kinetics in microscale. Chemical Engineering Science, 2010, 65, 2649-2655.	3.8	22
95	Self-Lubricating Polytetrafluoroethylene/Polyimide Blends Reinforced with Zinc Oxide Nanoparticles. Journal of Nanomaterials, 2015, 2015, 1-8.	2.7	22
96	Turning the solubility and lubricity of ionic liquids by absorbing CO 2. Tribology International, 2018, 121, 223-230.	5.9	22
97	Highly Crystalline Mesoporous TiO ₂ (B) Nanofibers. Journal of Physical Chemistry C, 2014, 118, 3049-3055.	3.1	21
98	CO ₂ Uptake Behavior of Supported Tetraethylenepentamine Sorbents. Energy & Fuels, 2016, 30, 5083-5091.	5.1	21
99	Localizing microwave heat by surface polarization of titanate nanostructures for enhanced catalytic reaction efficiency. Applied Catalysis B: Environmental, 2018, 227, 266-275.	20.2	21
100	Simple Physical Approach to Reducing Frictional and Adhesive Forces on a TiO ₂ Surface via Creating Heterogeneous Nanopores. Langmuir, 2012, 28, 15270-15277.	3.5	20
101	CO ₂ Absorption in Mixed Aqueous Solution of MDEA and Cholinium Glycinate. Energy & Fuels, 2017, 31, 7325-7333.	5.1	20
102	Thermodynamic analysis of CO2 separation from biogas with conventional ionic liquids. Applied Energy, 2018, 217, 75-87.	10.1	20
103	TiO ₂ Nanofoam–Nanotube Array for Surface-Enhanced Raman Scattering. ACS Applied Nano Materials, 2018, 1, 6563-6566.	5.0	20
104	Supported ionic liquid sorbents for CO2 capture from simulated flue-gas. Chinese Journal of Chemical Engineering, 2018, 26, 2377-2384.	3.5	20
105	A mini-review on the modeling of volatile organic compound adsorption in activated carbons: Equilibrium, dynamics, and heat effects. Chinese Journal of Chemical Engineering, 2021, 31, 153-163.	3.5	20
106	Protein adsorptive behavior on mesoporous titanium dioxide determined by geometrical topography. Chemical Engineering Science, 2014, 117, 146-155.	3.8	19
107	Temperature-dependent structural properties of water molecules confined in TiO2 nanoslits: Insights from molecular dynamics simulations. Fluid Phase Equilibria, 2016, 430, 169-177.	2.5	19
108	Influences of geometrical topography and surface chemistry on the stable immobilization of adenosine deaminase on mesoporous TiO 2. Chemical Engineering Science, 2016, 139, 142-151.	3.8	19

#	Article	IF	CITATIONS
109	CO ₂ Absorption in the Ionic Liquids Immobilized on Solid Surface by Molecular Dynamics Simulation. Langmuir, 2017, 33, 11658-11669.	3.5	19
110	AFM Study of pHâ€Ðependent Adhesion of Single Protein to TiO ₂ Surface. Advanced Materials Interfaces, 2019, 6, 1900411.	3.7	19
111	Determination of the small amount of proteins interacting with TiO2 nanotubes by AFM-measurement. Biomaterials, 2019, 192, 368-376.	11.4	19
112	DFT study of coverage-depended adsorption of NH3 on TiO2-B (100) surface. Physical Chemistry Chemical Physics, 2012, 14, 16618.	2.8	18
113	Flow resistance analysis of nanoconfined water in silt pores by molecular simulations: Effect of pore wall interfacial properties. Fluid Phase Equilibria, 2014, 362, 235-241.	2.5	18
114	Nanomaterial-oriented molecular simulations of ion behaviour in aqueous solution under nanoconfinement. Molecular Simulation, 2016, 42, 784-798.	2.0	18
115	Generalized Gibbs free energy of confined nanoparticles. AICHE Journal, 2017, 63, 4595-4603.	3.6	18
116	Effect of endogenous hydrogen utilization on improved methane production in an integrated microbial electrolysis cell and anaerobic digestion: Employing catalyzed stainless steel mesh cathode. Chinese Journal of Chemical Engineering, 2018, 26, 574-582.	3.5	18
117	Poly(ionic liquid)s as lubricant additives with insight into adsorption-lubrication relationship. Tribology International, 2022, 165, 107278.	5.9	18
118	A negative-carbon footprint process with mixed biomass feedstock maximizes conversion efficiency, product value and CO2 mitigation. Bioresource Technology, 2022, 351, 127004.	9.6	18
119	In-situ synthesized mesoporous TiO2-B/anatase microparticles: Improved anodes for lithium ion batteries. Chinese Journal of Chemical Engineering, 2015, 23, 583-589.	3.5	17
120	Confinement Phenomenon Effect on the CO ₂ Absorption Working Capacity in Ionic Liquids Immobilized into Porous Solid Supports. Langmuir, 2017, 33, 11719-11726.	3.5	17
121	CO2 separation using a hybrid choline-2-pyrrolidine-carboxylic acid/polyethylene glycol/water absorbent. Applied Energy, 2020, 257, 113962.	10.1	17
122	Interface‣trengthened Polyimide/Carbon Nanofibers Nanocomposites with Superior Mechanical and Tribological Properties. Macromolecular Chemistry and Physics, 2014, 215, 1407-1414.	2.2	15
123	Lubrication Behavior of Water Molecules Confined in TiO ₂ Nanoslits: A Molecular Dynamics Study. Journal of Chemical & Engineering Data, 2016, 61, 4023-4030.	1.9	15
124	Diffusion of CO ₂ /CH ₄ confined in narrow carbon nanotube bundles. Molecular Physics, 2016, 114, 2530-2540.	1.7	15
125	Tribological behaviors of carbon series additions reinforced <scp>CF/PTFE</scp> composites at high speed. Journal of Applied Polymer Science, 2016, 133, .	2.6	15
126	Right Way of Using Graphene Oxide Additives for Water-Lubricated PEEK: Adding in Polymer or Water?. Tribology Letters, 2018, 66, 1.	2.6	15

#	Article	IF	CITATIONS
127	Solvent effects on a derivative of 1,3,4-oxadiazole tautomerization reaction in water: A reaction density functional theory study. Chemical Engineering Science, 2020, 213, 115380.	3.8	15
128	Acetone adsorption on activated carbons: Roles of functional groups and humidity. Fluid Phase Equilibria, 2020, 521, 112645.	2.5	15
129	Dissociation of methanol on hydroxylated TiO2-B (100) surface: Insights from first principle DFT calculation. Catalysis Today, 2011, 165, 32-40.	4.4	14
130	Modelling interfacial properties of ionic liquids with ePC-SAFT combined with density gradient theory. Molecular Physics, 2016, 114, 2492-2499.	1.7	14
131	The effect of H2O2 desorption on achieving improved selectivity for direct synthesis of H2O2 over TiO2(B)/anatase supported Pd catalyst. Catalysis Communications, 2017, 89, 69-72.	3.3	14
132	Tribological Properties of Porous PEEK Composites Containing Ionic Liquid under Dry Friction Condition. Lubricants, 2017, 5, 19.	2.9	14
133	Multi-objective optimization and dynamic control of biogas pressurized water scrubbing process. Renewable Energy, 2020, 147, 2335-2344.	8.9	14
134	Heterogeneous interfacial engineering of Pd/TiO2 with controllable carbon content for improved direct synthesis efficiency of H2O2. Chinese Journal of Catalysis, 2020, 41, 312-321.	14.0	14
135	Interfacial structure and differential capacitance of ionic liquid/graphite interface: A perturbed-chain SAFT density functional theory study. Journal of Molecular Liquids, 2020, 310, 113199.	4.9	14
136	Versatile Ionic Gel Driven by Dual Hydrogen Bond Networks: Toward Advanced Lubrication and Self-Healing. ACS Applied Polymer Materials, 2021, 3, 5932-5941.	4.4	14
137	CO2-negative biomass conversion: An economic route with co-production of green hydrogen and highly porous carbon. Applied Energy, 2022, 311, 118685.	10.1	14
138	Efficient Molecular Approach to Quantifying Solvent-Mediated Interactions. Langmuir, 2017, 33, 11817-11824.	3.5	13
139	Carbon-Modified Mesoporous Anatase/TiO2(B) Whisker for Enhanced Activity in Direct Synthesis of Hydrogen Peroxide by Palladium. Catalysts, 2017, 7, 175.	3.5	13
140	Advanced Materialâ€Oriented Biomass Precise Reconstruction: A Review on Porous Carbon with Inherited Natural Structure and Created Artificial Structure by Postâ€Treatment. Macromolecular Bioscience, 2022, 22, e2100479.	4.1	13
141	Atomic force microscopy (AFM) study on potassium hexatitanate whisker (K2O·6TiO2). Journal of Materials Science, 2003, 38, 3641-3646.	3.7	12
142	Direct Electrochemistry and Electrocatalysis of Hemoglobin–TiO ₂ Whisker Film Modified Glassy Carbon Electrode. Electroanalysis, 2010, 22, 668-672.	2.9	12
143	Preparation and Characterization of Mesoporous MoO3/TiO2 Composite with High Surface Area by Self-Supporting and Ammonia Method. Catalysis Letters, 2012, 142, 480-485.	2.6	12
144	Molecular Behavior of Water on Titanium Dioxide Nanotubes: A Molecular Dynamics Simulation Study. Journal of Chemical & Engineering Data, 2016, 61, 4131-4138.	1.9	12

Χιλοήμα Lu

#	Article	IF	CITATIONS
145	Investigation of Structural, Thermal, and Dynamical Properties of Pd–Au–Pt Ternary Metal Nanoparticles Confined in Carbon Nanotubes Based on MD Simulation. Journal of Physical Chemistry C, 2017, 121, 12911-12920.	3.1	12
146	Flow-resistance analysis of nano-confined fluids inspired from liquid nano-lubrication: A review. Chinese Journal of Chemical Engineering, 2017, 25, 1552-1562.	3.5	12
147	Developing Electrolyte Perturbed-Chain Statistical Associating Fluid Theory Density Functional Theory for CO ₂ Separation by Confined Ionic Liquids. Journal of Physical Chemistry C, 2018, 122, 15464-15473.	3.1	12
148	Atomistic Insights into the Layered Microstructure and Time-Dependent Stability of [BMIM][PF ₆] Confined within the Meso-Slit of Carbon. Journal of Physical Chemistry B, 2019, 123, 6857-6869.	2.6	12
149	How to detect possible pitfalls in ePC-SAFT modelling: Extension to ionic liquids. Fluid Phase Equilibria, 2020, 519, 112641.	2.5	12
150	Atomistic insights into the effects of carbonyl oxygens in functionalized graphene nanopores on Ca2+/Na+ sieving. Carbon, 2020, 164, 305-316.	10.3	12
151	How to Detect Possible Pitfalls in ePC-SAFT Modeling. 2. Extension to Binary Mixtures of 96 Ionic Liquids with CO2, H2S, CO, O2, CH4, N2, and H2. Industrial & Engineering Chemistry Research, 2020, 59, 21579-21591.	3.7	12
152	Shape and size characterization of potassium titanate fibers by image analysis. Journal of Materials Science, 2004, 39, 469-476.	3.7	11
153	Changes in CNT-confined water structural properties induced by the variation in water molecule orientation. Molecular Simulation, 2012, 38, 1094-1102.	2.0	11
154	A study of tribological and mechanical properties of PTFE composites filled with surface treated K ₂ Ti ₆ O ₁₃ whisker. Journal of Applied Polymer Science, 2012, 124, 1456-1463.	2.6	11
155	A Novel Exploration of a Combination of Gambogic Acid with TiO2 Nanofibers: The Photodynamic Effect for HepG2 Cell Proliferation. Materials, 2014, 7, 6865-6878.	2.9	11
156	Dynamical coupling of ion adsorption with fluid flow in nanopores. AICHE Journal, 2021, 67, e17266.	3.6	11
157	Large-Scale Hydrothermal Synthesis of Twinned Rutile Titania. Journal of the American Ceramic Society, 2007, 90, 319-321.	3.8	10
158	Extra low friction coefficient caused by the formation of a solid-like layer: A new lubrication mechanism found through molecular simulation of the lubrication of MoS2 nanoslits. Chinese Journal of Chemical Engineering, 2018, 26, 2412-2419.	3.5	10
159	Molecular insights into the microstructure of ethanol/water binary mixtures confined within typical 2D nanoslits: The role of the adsorbed layers induced by different solid surfaces. Fluid Phase Equilibria, 2020, 509, 112452.	2.5	10
160	Molecular insight into wetting behavior of deep eutectic solvent droplets on ionic substrates: A molecular dynamics study. Journal of Molecular Liquids, 2020, 319, 114298.	4.9	10
161	Excellent Trace Detection of Proteins on TiO ₂ Nanotube Substrates through Novel Topography Optimization. Journal of Physical Chemistry C, 2020, 124, 27790-27800.	3.1	10
162	Durable polytetrafluoroethylene composites in harsh environments: Tribology and corrosion investigation. Journal of Applied Polymer Science, 2012, 124, 4307-4314.	2.6	9

#	Article	IF	CITATIONS
163	Unique Structures and Vibrational Spectra of Protic Ionic Liquids Confined in TiO ₂ Slits: The Role of Interfacial Hydrogen Bonds. Langmuir, 2018, 34, 13449-13458.	3.5	9
164	Effects of ionic hydration and hydrogen bonding on flow resistance of ionic aqueous solutions confined in molybdenum disulfide nanoslits: Insights from molecular dynamics simulations. Fluid Phase Equilibria, 2019, 489, 23-29.	2.5	9
165	Thermodynamic study on aqueous polyethylene glycol 200 solution and performance assessment for CO2 separation. Fluid Phase Equilibria, 2020, 504, 112336.	2.5	9
166	Excellent Protein Immobilization and Stability on Heterogeneous C–TiO ₂ Hybrid Nanostructures: A Single Protein AFM Study. Langmuir, 2020, 36, 9323-9332.	3.5	9
167	Mesoscience in supported nano-metal catalysts based on molecular thermodynamic modeling: A mini review and perspective. Chemical Engineering Science, 2021, 229, 116164.	3.8	9
168	Thermodynamic analysis and modification of Gibbs–Thomson equation for melting point depression of metal nanoparticles. Chinese Journal of Chemical Engineering, 2021, 31, 198-205.	3.5	9
169	Kinetics study and performance comparison of CO2 separation using aqueous choline-amino acid solutions. Separation and Purification Technology, 2021, 261, 118284.	7.9	9
170	Splitting behavior and structural transformation process of K2Ti6O13 whiskers under hydrothermal conditions. Journal of Materials Science, 2008, 43, 155-163.	3.7	8
171	Mechanistic Study of Protein Adsorption on Mesoporous TiO ₂ in Aqueous Buffer Solutions. Langmuir, 2019, 35, 11037-11047.	3.5	8
172	Computational screening carbon-based adsorbents for CH4 delivery capacity. Fluid Phase Equilibria, 2019, 494, 184-191.	2.5	8
173	Thermodynamic analysis of the theoretical energy consumption in the removal of organic contaminants by physical methods. Science China Chemistry, 2010, 53, 671-676.	8.2	7
174	Photosynthesis-inspired design approach of a liquid phase heterogeneous photoreactor. Green Chemistry, 2011, 13, 1784.	9.0	7
175	Methodology of non-equilibrium thermodynamics for kinetics research of CO2 capture by ionic liquids. Science China Chemistry, 2012, 55, 1079-1091.	8.2	7
176	Energy Consumption Analysis for CO2 Separation from Gas Mixtures with Liquid Absorbents. Energy Procedia, 2014, 61, 2695-2698.	1.8	7
177	Electric Fieldâ€Responsive Nanopores with Ion Selectivity: Controlling Based on Transport Resistance. Chemical Engineering and Technology, 2016, 39, 993-997.	1.5	7
178	Confined molecular motion across liquid/liquid interfaces in a triphasic reaction towards free-standing conductive polymer tube arrays. Journal of Materials Chemistry A, 2016, 4, 6290-6294.	10.3	7
179	Carbon coated Li4Ti5O12 fibers: Relying on the lithium diffusivity in TiO2–B crystal structure for high rate lithium battery. Journal of Alloys and Compounds, 2017, 721, 545-553.	5.5	7
180	Accelerate the ePC-SAFT-DFT Calculation with the Chebyshev Pseudospectral Collocation Method. Industrial & Engineering Chemistry Research, 2021, 60, 9269-9285.	3.7	7

#	Article	IF	CITATIONS
181	Critical Role of Carbonized Cellulose in the Evolution of Highly Porous Biocarbon: Seeing the Structural and Compositional Changes of Spent Mushroom Substrate by Deconvoluted Thermogravimetric Analysis. Industrial & Engineering Chemistry Research, 2020, 59, 22541-22548.	3.7	7
182	Hollow IF-MoS2/r-GO Nanocomposite Filled Polyimide Coating with Improved Mechanical, Thermal and Tribological Properties. Coatings, 2021, 11, 25.	2.6	7
183	Mineralization of Trace Nitro/Chloro/Methyl/Amino-Aromatic Contaminants in Wastewaters by Advanced Oxidation Processes. Industrial & Engineering Chemistry Research, 2010, 49, 6243-6249.	3.7	6
184	Exploration on the structure, stability, and isomerization of planar C _{<i>n</i>} B ₅ (<i>n</i> = 1â^'7) clusters. International Journal of Quantum Chemistry, 2013, 113, 2514-2522.	2.0	6
185	Adsorption of N-Butane/I-Butane in Zeolites: Simulation and Theory Study. Separation Science and Technology, 2014, 49, 1215-1226.	2.5	6
186	Molecular dynamics simulation of melting and crystallization processes of polyethylene clusters confined in armchair single-walled carbon nanotubes. Journal of Molecular Modeling, 2015, 21, 9.	1.8	6
187	Abnormal change of melting points of gold nanoparticles confined between two-layer graphene nanosheets. RSC Advances, 2016, 6, 108343-108346.	3.6	6
188	Progress in molecular-simulation-based research on the effects of interface-induced fluid microstructures on flow resistance. Chinese Journal of Chemical Engineering, 2019, 27, 1403-1415.	3.5	6
189	Study of CO2 absorption/desorption behaviors in aqueous (2-hydroxyethyl)-trimethyl-ammonium (S)-2-pyrrolidine-carboxylic acid salt ([Cho][Pro]) + K2CO3 solutions. International Journal of Greenhouse Gas Control, 2019, 83, 51-60.	4.6	6
190	A novel interfacial thermodynamic model for predicting solubility of nanoparticles coated by stabilizers. Chinese Journal of Chemical Engineering, 2021, 31, 103-112.	3.5	6
191	Feasibility of Solar Updraft Towers as Photocatalytic Reactors for Removal of Atmospheric Methane–The Role of Catalysts and Rate Limiting Steps. Frontiers in Chemistry, 2021, 9, 745347.	3.6	6
192	Thermal analysis of hydrogen titanate nanotubes prepared by potassium dititanate with water vapour treatment. Journal of Thermal Analysis and Calorimetry, 2012, 110, 671-675.	3.6	5
193	Hydrophilicity effect on CO ₂ /CH ₄ separation using carbon nanotube membranes: insights from molecular simulation. Molecular Simulation, 2017, 43, 502-509.	2.0	5
194	Wetting control through topography and surface hydrophilic/hydrophobic property changes by coarse grained simulation. Molecular Simulation, 2017, 43, 1202-1208.	2.0	5
195	Pd catalysts supported on rGO-TiO 2 composites for direct synthesis of H 2 O 2 : Modification of Pd 2+ /Pd 0 ratio and hydrophilic property. Chinese Journal of Chemical Engineering, 2018, 26, 534-539.	3.5	5
196	Poly(alkylimidazolium bis(trifluoromethylsulfonyl)imide)â€Based Polymerized Ionic Liquids: A Potential Highâ€Performance Lubricating Grease. Advanced Materials Interfaces, 2019, 6, 1801796.	3.7	5
197	Modeling Interfacial Properties with Spot-DCT-ePC-SAFT for Binary Mixtures Including Ionic Liquid-Based Systems. Industrial & Engineering Chemistry Research, 2021, 60, 4484-4497.	3.7	5
198	Modeling interfacial properties of ionic liquids with ePC-SAFT combined with density gradient theory. Fluid Phase Equilibria, 2021, 536, 112984.	2.5	5

#	Article	IF	CITATIONS
199	CO2 absorption using a hybrid 1-hexyl-3-methylimidazolium bis(trifluoromethylsulfonyl)imide/titanium dioxide/polyethylene glycol absorbent. Fluid Phase Equilibria, 2021, 538, 113011.	2.5	5
200	Partition and selectivity of electrolytes in cylindrical nanopores with heterogeneous surface charge. Journal of Molecular Liquids, 2021, 340, 116839.	4.9	5
201	Some Insight into Stability of Amorphous Poly(ethylene glycol) Dimethyl Ether Polymers Based on Molecular Dynamics Simulations. Journal of Physical Chemistry Letters, 2013, 4, 1718-1722.	4.6	4
202	Adsorption of binary CO ₂ /CH ₄ mixtures using carbon nanotubes: Effects of confinement and surface functionalization. Separation Science and Technology, 2016, 51, 1079-1092.	2.5	4
203	Interfacial Engineering of NiMo/Mesoporous TiO2 Catalyst with Carbon for Enhanced Hydrodesulfurization Performance. Catalysis Letters, 2018, 148, 992-1002.	2.6	4
204	Improved CO2 separation performance of aqueous choline-glycine solution by partially replacing water with polyethylene glycol. Fluid Phase Equilibria, 2019, 495, 12-20.	2.5	4
205	Molecular insight into flow resistance of choline chloride/urea confined in ionic model nanoslits. Fluid Phase Equilibria, 2021, 533, 112934.	2.5	4
206	Simultaneous representation of thermodynamic properties and viscosities of ILs/DESs+co-solvent systems by Eyring-NRTL model. Fluid Phase Equilibria, 2021, 547, 113176.	2.5	4
207	Accelerate the Electrolyte Perturbed-Chain Statistical Associating Fluid Theory–Density Functional Theory Calculation With the Chebyshev Pseudo-Spectral Collocation Method. Part II. Spherical Geometry and Anderson Mixing. Frontiers in Chemistry, 2021, 9, 801551.	3.6	4
208	Effect of surface roughness on partition of ionic liquids in nanopores by a perturbed-chain SAFT density functional theory. Journal of Chemical Physics, 2022, 157, .	3.0	4
209	Modeling mass transfer of CO2 in brine at high pressures by chemical potential gradient. Science China Chemistry, 2013, 56, 821-830.	8.2	3
210	Shape-controllable synthesis of CeO2 particles in CO2-expanded ethanol towards CO oxidation application. RSC Advances, 2013, 3, 5302.	3.6	3
211	Determination of the ion exchange process of K ₂ Ti ₄ O ₉ fibers at constant pH and modeling with statistical rate theory. RSC Advances, 2015, 5, 73474-73480.	3.6	3
212	Biomethane storage in activated carbons: a grand canonical Monte Carlo simulation study. Molecular Simulation, 2017, 43, 1142-1152.	2.0	3
213	Energy-consumption analysis of carbon-based material for CO2 capture process. Fluid Phase Equilibria, 2020, 510, 112504.	2.5	3
214	Mass Transfer Behavior of Methane in Porous Carbon Materials. AICHE Journal, 0, , e17521.	3.6	3
215	Molecular insights on Ca2+/Na+ separation via graphene-based nanopores: The role of electrostatic interactions to ionic dehydration. Chinese Journal of Chemical Engineering, 2022, 41, 220-229.	3.5	3
216	Atomistic insight into the lubrication of glycerol aqueous solution: The role of the solid interfaceâ€induced microstructure of fluid molecules. AICHE Journal, 0, , .	3.6	3

#	Article	IF	CITATIONS
217	Modeling of specific structure crystallization coupling with dissolution. Frontiers of Chemical Engineering in China, 2010, 4, 52-56.	0.6	2
218	Effect of dimethyl carbonate on the behavior of water confined in carbon nanotube. Chinese Journal of Chemical Engineering, 2021, 31, 177-185.	3.5	2
219	Cycling pressure-switching process enriches micropores in activated carbon by accelerating reactive gas internal diffusion in porous channels. Sustainable Materials and Technologies, 2021, 28, e00248.	3.3	2
220	Molecular Understanding of the Solid Interface-Induced Microstructures of 1-Hexyl-3-methylimidazolium Bis(trifluoromethylsulfonyl)imide in Gas Absorption. Industrial & Engineering Chemistry Research, 2022, 61, 3754-3765.	3.7	2
221	Surface Structure and Interaction of Surface/Interface Probed by Mesoscale Simulations and Experiments. Advances in Chemical Engineering, 2015, 47, 85-162.	0.9	1
222	Novel Solvent for CO2 Capture. Energy Procedia, 2019, 158, 5124-5129.	1.8	1
223	Naturally dispersed ash components in bio-carbon composites: integrated ammonia nitrogen removal and specific surface area augment. Biomass Conversion and Biorefinery, 0, , 1.	4.6	1
224	Screening ionic liquids for developing advanced immobilization technology for CO2 separation. Frontiers in Chemistry, 0, 10, .	3.6	1
225	Theoretical limiting concentration for mineralization of trichloromethane and dichloromethane in aqueous solutions by AOPs. Science China Chemistry, 2011, 54, 559-564.	8.2	0
226	Large-Scale Fabrication of Rutile TiO2 with 3D Hierarchical Flower-Like Morphology. Journal of Nanoscience and Nanotechnology, 2016, 16, 12991-12995.	0.9	0
227	Biogas upgrading using single-walled carbon nanotubes by molecular simulation. Molecular Simulation, 2017, 43, 1034-1044.	2.0	0
228	<i>In Situ</i> Template-Synthesis of Hollow CeO ₂ Nanobeads in scCO ₂ with Improved Catalytic Activity Towards CO Oxidation. Journal of Nanoscience and Nanotechnology, 2018, 18, 2068-2071.	0.9	0
229	A NEW THERMODYNAMIC MODEL FOR AQUEOUS ALKALI-EARTH METAL SOLUTION BASED ON THE SYNERGISTIC ACTION OF ASSOCIATION AND HYDRATION UNDER SUPERCRITICAL CONDITIONS. , 2004, , .		0
230	Viscous behavior of 1-hexyl-methylimidazolium bis(trifluoromethylsulfonyl)imide/titanium dioxide/polyethylene glycol. Chinese Journal of Chemical Engineering, 2023, 54, 280-287.	3.5	0